

Nonstationary Deformation and Failure of Composite Shells

V. N. Bakulin^{1*} and A. V. Ostriuk^{2**}

¹*Institute of Applied Mechanics, Russian Academy of Sciences,
GSP-1, V-334, Leninskii pr-t 32A, Moscow, 117334 Russia*

²*Institute for Problems of Chemical Physics, Russian Academy of Sciences,
Akad. Semenova 1, Chernogolovka, Moscow oblast, 142432 Russia*

Received December 12, 2005

Abstract—We present the results of experimental studies of the strength of composite shells of cotton winding under the action of a lateral nonstationary load. We briefly describe devices generating pressure pulses of complicated space-time profile and the tools for measuring the parameters of the original object response to dynamic and pulse loadings. We study the influence of the action duration and the pressure application domain dimensions on the character of failure of empty and filled shells. We show that, at the shell stage of deformation, for the failure criterion one can take the moment at which the maximal circular strains attain some limit level (of the order of 2%). We propose some relations for estimating the maximal circular strain in terms of the shell characteristics and the load parameters.

DOI: 10.3103/S0025654408040110

1. INTRODUCTION

The wide use of composite materials in bearing thin-walled constructions of spacecraft raised a significant interest in studies of the character and characteristics of their strain and failure [1]. The understanding that it is necessary to preserve the working ability of these structures under the conditions of intensive pulse and dynamic loads of various physical nature [1–7] required the development of special experimental setups [2, 8] for testing full-scale elements of spacecraft structures under the modeled flight conditions [9, 10].

The goal in this paper is to represent several experimental results of studies of the action of the lateral nonstationary load on composite shells of cotton winding [1]. These results are part of the data obtained in the framework of the general methods [11, 12] for testing the strength of composite shells under the mechanical action of radiation and can illustrate the variety and complexity of the problems arising when analyzing the strength of bearing elements of spacecraft structures under nontraditional forms of actions with high energy density.

2. DEVICES FOR MODELING THE MECHANICAL ACTION OF RADIATION

It is impossible to study the aftereffects of mechanical action of radiation on spacecraft structure elements experimentally by exposing them to direct radiation, because there are no powerful laboratory radiation sources that can generate the required energy densities on surfaces of dimensions of the order of several meters [8]. In a majority of cases, it is also impossible to obtain sufficiently reliable results by modeling methods [13], because the requirements that the criterion parameters coincide for the model and for the full-scale structure are practically reduced to the requirements that the latter be identical in the absolute dimensions and material properties. For example, if the fuel charge of a geometrically similar model of a spacecraft solid-fuel jet engine has characteristic dimensions that do not exceed the critical detonation dimension, then it is absolutely impossible to model the detonation caused by the action of the mechanical radiation pulse, although it can occur for the full-scale engine. Similar difficulties arise in the attempts to model nonstationary failures of thin-walled composite bodies of

*E-mail: vbak@yandex.ru

**E-mail: ostriuk@ficp.ac.ru

Table 1

Type of explosive assembly	Load parameters		Objective (modeled operation modes)
	τ_p	I_p	
Contact sector charge	$10^{-6} - 10^{-5}$	0.8 – 5	UVR or XRR monopulse action
Contact laser-supported detonation charge	$2 \cdot 10^{-7} - 10^{-6}$	0.05 – 2	XRR monopulse action
Equidistant surface charge	$10^{-5} - 2 \cdot 10^{-4}$	0.3 – 3	Monopulse action of visible or IR radiation in the air
Volume-distributed charge	$10^{-4} - 5 \cdot 10^{-4}$	0.1 – 2	Monopulse action of visible or IR radiation in the air
Cumulative volume-distributed charge	$10^{-4} - 5 \cdot 10^{-4}$	0.1 – 2	Monopulse cumulative action of visible or IR radiations in the air
Shock tube of explosive action	$5 \cdot 10^{-5} - 2 \cdot 10^{-4}$	0.5 – 2	Pulse-frequency resonance action of visible or IR radiation in the air
Shock tube of explosive action with packing	$5 \cdot 10^{-5} - 2 \cdot 10^{-4}$	0.5 – 2	Pulse-frequency action of visible or IR radiation with complicated spatial profile in the air
System of rotation charges	$10^{-4} - 2 \cdot 10^{-4}$	0.5 – 2	Multiple action of radiation on high-temperature flows

cotton winding. The condition that the body and model relative thicknesses h/R (where h and R are the thickness and the characteristic radius of curvature of the shell) must coincide for the same thickness of the reinforcing cotton results in a decrease in the number of the model reinforcement layers, which, in turn, distorts the character and sequence of failures of these layers. Therefore, at present, the main methods for studying the mechanical action of radiation aftereffects are tests of full-scale spacecraft structures under nonstationary loading by gasdynamic devices reproducing the mechanical action of pulse radiation [8–12, 14]. The characteristics of these devices are shown in Table 1 (where τ_p s is the load duration; I_p kPa·s is the pressure pulse; UVR is the ultraviolet radiation; XRR is the X-ray radiation; and IR is the infrared radiation).

3. OBJECTS OF STUDY

For the objects of experimental studies we take the shells of “cocoon” type with flange joints at the ends [1], which are widely used in spacecraft structures. The force construction consists of the one-piece-winded bottoms and the cylindrical part formed by continuous winding of the SVM organoplastic braid and the EDT-10 binding; moreover, the bottoms are obtained only by winding the spiral layer and the cylindrical part is reinforced by coil layers. The spiral layer winding makes an angle of 22.5° with the reinforcement scheme from the shell internal radius: PKhPKh. The flanges made of 30KhGSA steel are built in the shell end faces. The air-tightness is ensured by a rubber layer applied to the entire shell surface, and the filler is fastened to the shell by an adhesion layer. To ensure the operation of the shell under significant axial loads, some glass-fiber plastic joint units are additionally winded. The dimensionless parameters characterizing the geometry of the tested shells are $\bar{h} = h/R = 0.012$, and $L/R = 1.85$ (where L , R , and h are the length, radius, and thickness of the cylindrical part of the shell). All tested shells were made according to the same technology and endured the same regimes of thermal treatment, which allows us to perform the complex study of their reaction to unsteady loads.

4. MEASUREMENT OF RESPONSE PARAMETERS

An essential part of any testing methodology consists of methods for measuring the parameters of the tested object response to the external action. In studying the processes in the structure elements caused by pulse loads, all the measured parameters can be conventionally divided into two groups. The first group characterizes the behavior of the tested structure during nonstationary processes caused in it by an external action. The second group of parameters characterizes the further state of the object during its operation after the nonstationary action. The methods for measuring the parameters of the second group are chosen and developed at the stage of the spacecraft tests for its functional abilities and without any

external actions taken into account. Therefore, the parameters of this group are specific for each object (for example, in the case of tests of operating engines [15], they are the driving force, the pressure at different points of the combustion chamber, and the engine body temperature); they are not directly related to tests for nonstationary loads, and the methods for their measurement are not discussed. (They can be taken from the methodology of appropriate functional tests for spacecraft elements.)

The main parameters in the first group are stresses and mass velocities, nonstationary strains, overloads at important spacecraft units, deflections in the process of deformation, and the residual deflections under failure or elastoplastic strain of the structure (in the case of metal bearing layer of the structure).

The methods for measuring stresses and mass velocities in the structure fragments are the most developed methods [16–20]. The stresses are registered by film piezotransducers whose main element is the organic polycrystal film of thickness $0.5\text{--}5\ \mu\text{m}$ with a sensitive element with dimensions $1 \times 1\ \text{mm}^2$, specific capacity $40\text{--}60\ \text{pF}/\text{mm}^2$, internal resistance $10\ \text{G}\Omega$, and measurement range from several atmospheres to thousands of atmospheres [17]. The transducer is characterized by high sensitivity, wide measurement range, selectivity to some components of the stress tensor, and the possibility of being mounted between the structure layers in the process of the composition shell winding. By mounting piezofilms at different places, one can monitor the actual mechanical load, determine the shock wave decay over the shell thickness, and specify the existing criteria for chipping-off.

The mass velocity was measured by the electromagnetic method proposed by E. K. Zavoiskii and developed in [18, 19]. Π -shaped transducers made of thin copper foil ($\delta \approx 0.03\ \text{mm}$) whose beam is the operating part (of length of the order of $2.5\ \text{mm}$) are placed in the specimen cross-sections at equal distances from the loaded surface. The specimen with transducers is placed in a constant magnetic field so that the directions of the magnetic induction lines, the velocities of the shock wave front, and the operating parts of the transducers are mutually perpendicular. As a result of the wave processes, the transducer is set in motion and intersects the magnetic lines. In this case, by the Faraday electromagnetic induction law, the transducer velocity equal to the velocity of the matter (the transducers are assumed to be inertia-free) is proportional to the electromotive force induced in the foil, and by registering the electromotive force in the foil by a pulse oscillograph, one can readily determine the velocity itself as a function of time.

The unsteady strains are, as a rule, measured by the electrotenometric method according to the balanced ordinary bridge scheme. For the measurement transducers, the strain gauges are usually used, which permit measuring the relative unsteady strain up to 4% with accuracy of at most 15% (for example, the strain gauges of KB-10-200 type). In the loading region, each internal strain gauge is located opposite to the external strain gauge, so that the output signals from the transducers could be summed and subtracted, which permits obtaining the characteristics of the membrane and flexural strains.

The overloads are measured by high-frequency vibration-surviving transducers with a high coefficient of transformation and maximal values of measured accelerations $\leq 10^4\ \text{g}$ (for example, the ADP-10-1 transducer whose measurement error does not exceed 20%).

To measure deflexions in the process of deformation, it is expedient to use induction transducers, and to measure the maximal deflections, the crashers made of different materials (lead, copper). The residual deflection is fixed by straightforward measurements of the structure internal dimensions before and after the tests by using micrometer internal gauges or indicator devices, which, together with special devices, permit ensuring the absolute accuracy of measurements not less than $\pm 0.1\ \text{mm}$.

5. INFLUENCE OF THE SPACE-TIME DISTRIBUTION OF THE LOAD

First, the composite shells were under the action of a load with parameters that do not lead to their damage (a shock tube of explosive action (STEA) with pressure pulse $I_p = 0.5\ \text{kPa}\cdot\text{s}$ of duration $\tau_p = 100\ \mu\text{s}$ and load spot diameter $R_p = 200\ \text{mm}$ equal to the dimension of the shell transverse cross-section). The shell was freely suspended on ropes or rigidly fixed at a distance from the nozzle exit section of the shock tube of explosive action. The tests showed that the shell fixation conditions significantly affect its stress-strain state. But in both cases (for the freely suspended and rigidly fixed shells), the maximal circular strains turned out to be twice as large as the longitudinal strains. Although there is a significant variation in the shape (the maximal deflection was equal to 0.2 radius), the shells did not have visible damages caused by loading and completely regained their shape after the strain.

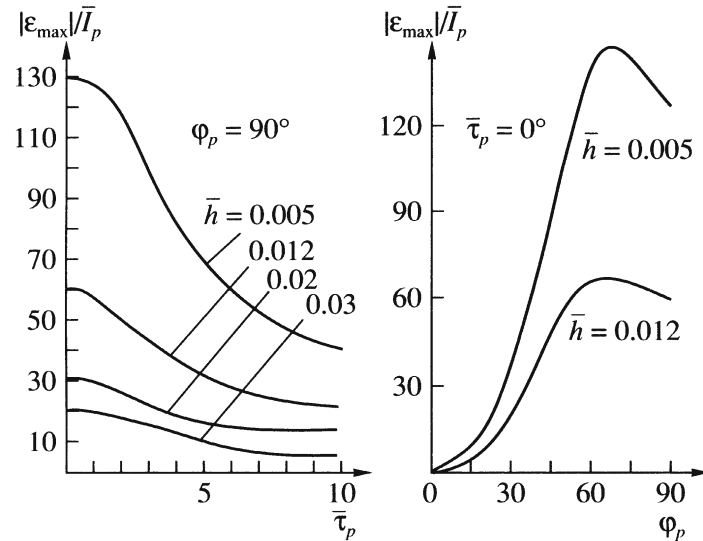


Fig. 1.

An analysis of the strain development in time shows that the strain has the character of complex multifrequency vibration processes whose duration is more than by an order of magnitude greater than the load duration and whose amplitude attains values of 1.7%. At the beginning of deformation, there are radial vibrations with predominating compressing stresses over the entire thickness of the structure. Some time after the load stops acting (in our case, $t = 500 \mu\text{s}$), one observes a gradual and then accelerating increase in the circular flexural strains (in this case, the signals from the strain gauges on the external and internal sides of the shell are of opposite polarity) with the maximum deflection at $t = 1.2 \text{ ms}$.

Since the circular strains are significantly greater than the longitudinal ones and the shell strain is elastic until the failure, for the strength criterion one can take the condition that the maximum is attained by the circular strains of some critical level (in the case of nonstationary loading, as experimental results show, this level is of the order of 2%). The fact that the circular strains are predominating and the strength criterion chosen above permit using the infinite elastic cylindrical shell model as the structure computational model. Then, as follows from the equations describing such a model, the value of the maximal circular strain depend on seven parameters: the shell radius R , the tensional and flexural rigidities B and D , the mass surface density m , and the parameters I_p , τ_p , and φ_p (the angular dimension of the loading domain). Since only three of these parameters have independent dimensions, it follows from the π -theorem [13] that the maximal circular strain ε_{\max} is determined by four dimensionless complexes (for a homogeneous shell of thickness h , the parameter \bar{h} coincides with the relative thickness h/R):

$$\varepsilon_{\max} = \bar{I}_p f(\bar{h}, \bar{\tau}_p, \bar{\varphi}_p), \quad \bar{h} = \sqrt{\frac{12D}{BR^2}}, \quad \bar{I}_p = \frac{I_p \bar{h}}{\sqrt{mB}}, \quad \bar{\tau}_p = \frac{\tau_p \sqrt{B/m}}{R}. \quad (5.1)$$

Relation (5.1) takes into account the fact that, because of the elastic behavior of the shell, the value of strain is proportional to the pressure pulse. Some computational results for the dependence $f(\bar{h}, \bar{\tau}_p, \bar{\varphi}_p)$ obtained by the method of numerical modeling of the shell strains [4] are shown in Fig. 1.

They permit estimating the maximal circular strains of multilayer elastic composite shells. In the first approximation, the existence of flight thermal loads can also be taken into account. To take the trajectory inhomogeneous heating of the shell into account, in calculating the rigidities contained in (5.1) one must assume that the strain characteristics of the layers are given functions of temperature. The influence of the internal pressure in the shell can be estimated approximately by summing the initial static and maximal dynamic strains.

The experimental distributions of deflections along the angular coordinate shows that, at the beginning of strain in the peripheral part of the load spot (for $\varphi_p > 40^\circ$), the shell moves towards the acting mechanical pressure. Therefore, as the load spot dimensions φ_p decrease, peripheral buckling

becomes easier and an increase in the maximal strain is observed, although the integral pulse decreases. As follows from Fig. 1, only for the angles $\varphi_p \leq 60^\circ$, the decrease in the integral pulse predominates and the maximal circular strain decreases. As a result, the loading not over the entire surface but over a local spot covering one-third of the surface is most dangerous.

Figure 2 presents the results of comparison of the estimates of maximal circular strains (in percents) obtained by the above dependences and by experimental data under the total one-sided loading ($\varphi_p = 90^\circ$) for different durations ($\tau_p = 10, 100, 300 \mu\text{s}$, $\bar{h} = 0.012$, and $\varphi_p = 90^\circ$) and pressure pulses (I_p kPa·s). Although the agreement is satisfactory, we note that a decrease in the duration results in a change in the character of the failure, which is now caused not by the shell flexural strains but by the wave processes over the thickness of the structure. For example, Fig. 3 shows the variation in the character of the shell failure depending on the space-time distribution of the load ((a) the case of monopulse load with $\tau_p = 1 \mu\text{s}$; (b) the case of double load by pulses of duration $\tau_p = 100 \mu\text{s}$ of each of them and with the time interval $\tau_p = 650 \mu\text{s}$ between them; (c) the case of cumulative monopulse load with $\tau_p = 100 \mu\text{s}$) under a fixed total pressure pulse $I_p = 1$ kPa·s. One can see that, for the duration $\tau_p = 1 \mu\text{s}$, the destructions are most severe and have the form of material chipping-off separation. Of course, in this case, it is not correct to use the failure criterion in terms of the maximal circular strains, and it is necessary to resort to the methods for calculating the wave processes and the corresponding criteria for chipping-off damages [20].

Note that the level of destructions under the cumulative actions (also shown in Fig. 3) is high even in the case where the load duration is sufficiently long ($\tau_p = 100 \mu\text{s}$) and the wave processes do not play a significant role. In this case, the load was created by the STEA with packing mounted in its nozzle to profile the loads, which, in the framework of the same device, permits simultaneously simulating the pulse-frequency and the space-inhomogeneous action, which initiates the resonance and cumulative effects in the structure. Thus, as the experimental results show, the version of loading by the pressure waves convergent at the structure surface is much more dangerous for thin-walled composite structures than the one-sided dynamic loading without cumulation.

6. TESTS OF FILLED SHELLS

As the results of numerous tests show, the existence of a filler with an internal channel significantly affects the shell responses to unsteady loads with the tendency to decrease these responses (in particular, the deflection decreases significantly) and, as a rule, for sufficiently large thickness of the arch (of the order of several shell thicknesses and more), the violation of the normal operation of the structure element occurs as a result of wave destructions of the filler, which can be calculated by using several known numerical methods [21, 22]. In the practically important case, where the filler rigidity is much less than the shell rigidity (for example, in the case of solid-fuel jet engines), if the arch thickness is less than several shell thicknesses, then the circular strains can be estimated by using the reduced relations (5.1) by considering the filler as an associated mass and taking it into account as an increase in the mass surface density m .

The filled shells were tested for different fillers with significantly different densities. The following fillers were used in the experiments: foamed plastic (of mark PPU-KF with density $\rho_s = 0.2 \text{ g/cm}^3$), rubber (hermetic of mark 31G24 with density $\rho_s = 1.3 \text{ g/cm}^3$), and solid fuel imitator ($\rho_s = 1.8 \text{ g/cm}^3$). In the interior of the filler, a channel of relative radius $r_s/R \leq 0.2$ was made along the shell axis, which permits estimating the filler state after the loading and generates a tensile wave after the reflection of the compression wave coming from the surface. The experiments show that, for the above filler materials, the maximal shell strain decreases by a factor from 1.5 to 5 as the density of the fillers increases. Thus, the filler prevents the shells under study from the destruction by load pulses with parameters $I_p \leq 1$ kPa·s and $\tau_p > 100 \mu\text{s}$ (the empty shells with $I_p \leq 1$ kPa·s and $\tau_p = 100 \mu\text{s}$ have significantly more severe damages). The filled shells are deformed at a smaller frequency, the vibration amplitude decays much faster than that of the empty shells (the time of decay is $3 \mu\text{s}$ and $40 \mu\text{s}$, respectively), and the maximal strains occur later. As the pulse duration decreases to $10 \mu\text{s}$, the shell destruction occurs with formation of cavities of depth up to two thicknesses and separation in the loading region. In this case, the shell has residual strains, but there are no cotton breaks in the composite material ribbons. In the domain of the filler adjacent to the shell, a region of tensile stresses arises, which results in the separation of the filler from the body (Fig. 4 a).

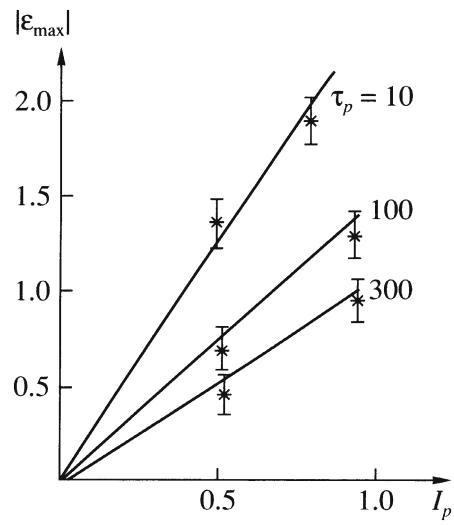


Fig. 2.

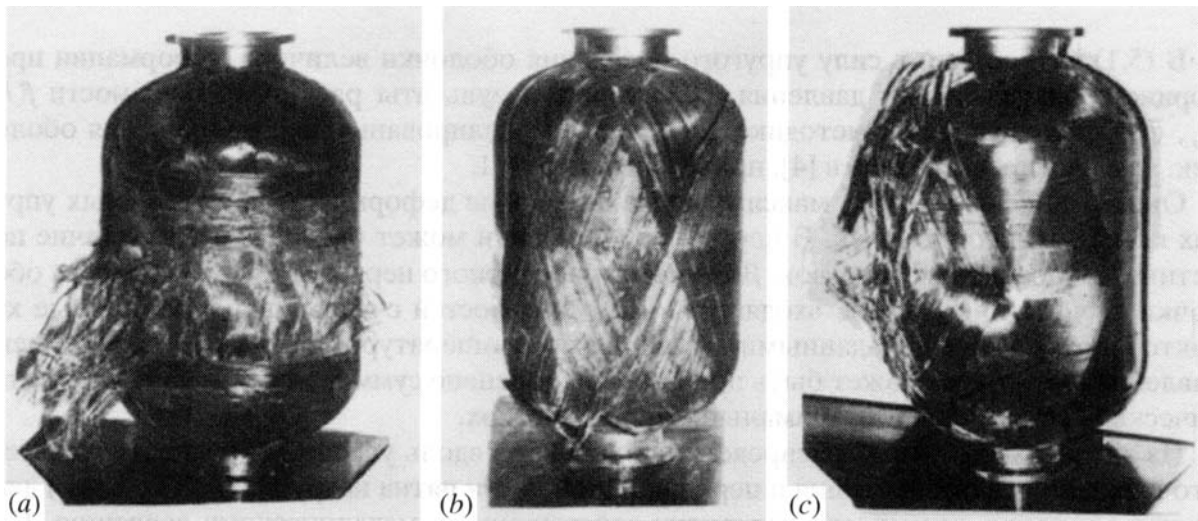


Fig. 3.

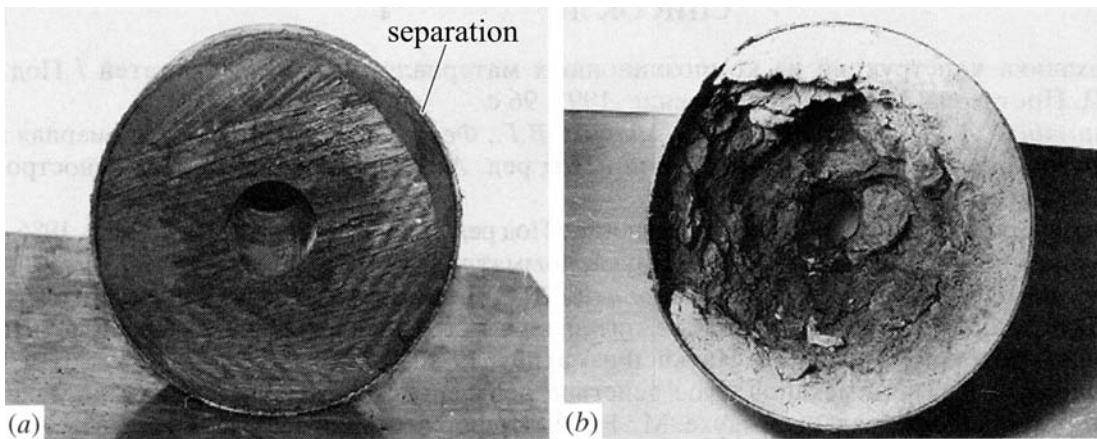


Fig. 4.

More severe destructions in the filler are caused by the tensile wave formed by reflecting from the free surface of the internal channel (Fig. 4*b*). We note that, in the tests of filled shells, the shell separation does not occur on their internal side, because the filler prevents the tensile wave from rather intensive reflections from the contact boundary.

ACKNOWLEDGMENTS

The research was financially supported by the Russian Foundation for Basic Research (project no. 08-01-00822).

REFERENCES

1. V. D. Protasov (Editor), *Mechanics of Constructions Made of Composite Materials. Collection of Scientific Papers* (Mashinostroenie, Moscow, 1992) [in Russian].
2. A. V. Karmishin, E. D. Skuratov, V. G. Startsev, and V. A. Feldshtein, *Unsteady Aeroelasticity of Thin-Walled Constructions*, Ed. by A. V. Karmishin (Mashinostroenie, Moscow, 1982) [in Russian].
3. V. P. Velikhov et al. (Editors), *Cosmic Weapon: Security Dilemma* (Mir, Moscow, 1986) [in Russian].
4. *Physics of Nuclear Explosion*, Vol. 2 (Nauka, Moscow, 1997) [in Russian].
5. V. N. Bakulin, I. F. Obraztsov, and V. A. Potopakhin, *Dynamical Problems of Nonlinear Theory of Multilayer Shells: Actions of Intensive Thermal Force Loads and Concentrated Energy Fluxes* (Nauka, Fizmatlit, Moscow, 1998) [in Russian].
6. I. F. Ostriuk, *Thermomechanical Actions of XR Radiation on Multilayer Heterogeneous Obstacles in the Air* (NTTs "Informatika", Moscow, 2003) [in Russian].
7. V. N. Bakulin and I. F. Ostriuk, "Computation-Experimental Study of Radiation Mechanical Action on Composite Elements of Constructions of Space Vehicles under Flight Conditions," in *Mechanics of Composite Materials and Constructions*, Vol. 5, No. 4 (IPRIM RAN, Moscow, 1999), pp. 151–166.
8. V. M. Loborev, I. F. Ostriuk, V. P. Petrovskii, and A.A. Cheprunov, *Methods for Modeling Radiation Mechanical Action on Materials and Constructions*, Collection of Scientific Papers, No. 1 (TsFTI, MO, RF, Sergiev Posad, 1997) [in Russian].
9. I. F. Ostriuk, V. N. Bakulin, and A.A. Cheprunov, "Experimental Methods for Studying the Radiation Mechanical Action on Thin-Walled Composite Bodies of Constructions," in *Problems of Strength and Plasticity* (Izd. Nizhegorod. Univ., Nizhnii Novgorod, 2000), pp. 117–121 [in Russian].
10. I. F. Ostriuk, "Computation-Experimental Prediction of Aftereffects of Mechanical Action of XR Radiation on the Bodies of Space Vehicles," in *Constructions Made of Composite Materials*, No. 1 (2002), pp. 41–45 [in Russian].
11. I. F. Ostriuk and V. P. Petrovskii, "Experimental Methods for Studying the Operation Ability of Composite Constructions under the Action of Unsteady Loads," in *Constructions Made of Composite Materials*, No. 1 (1996), pp. 3–9 [in Russian].
12. I. F. Ostriuk, "Computation-Experimental Method for Studying the Strength of Thin-Walled Composite Constructions under the Mechanical Action of Pulse Radiation," in *14th Jubilee Petersburg Readings in the Strength Problem. Collection of Theses* (St.Petersburg, 2003) [in Russian].
13. L. I. Sedov, *Similarity Methods and Dimensions in Mechanics* (Nauka, Moscow, 1981) [in Russian].
14. I. F. Ostriuk, V. P. Petrovskii, and A. D. Zaitsev, "Gas Dynamics Devices for Generating Unsteady Loads with Complicated Space-Time Profile," in *Constructions Made of Composite Materials*, Nos. 3–4 (1996), pp. 3–12 [in Russian].
15. I. F. Ostriuk and V. P. Petrovskii, "Firing Bench-Tests on Strength of Solid-Fuel Rocket Engines under the Action of Lateral Short-Time Load," *Khim. Fiz.* **14** (1), 11–17 (1995).
16. R. A. Graham, F. W. Nellson, and W. B. Benedick, "Piezoelectric Current from Shock Loaded Quarts/ A Submicrosecond Stress Gauge," *Appl. Phys.* **36** (5), 1775–1783 (1965).
17. A. A. Cheprunov and N. I. Shentsev, "Experimental Determination of Parameters of Hybrid Media under Shock-Wave Loads," *Mat. Modelirovanie* **4** (12), 167–173 (1992).
18. A. N. Dremin and P. F. Pokhil, "Parameters of the Trotyl, Cyclonite, Nitroglycerine, and Nitromethane Detonation Wave," *Dokl. Akad. Nauk SSSR* **128** (5), 989–991 (1959).
19. P. F. Pokhil, A. D. Zaitsev, and K. K. Shvedov, "Electromagnetic Method for Measuring the Velocity of Explosion Products," *Dokl. Akad. Nauk SSSR* **132** (6), 1339–1340 (1960).
20. G. I. Kanel, S. V. Razorenov, A. V. Utkin, and V. E. Fortov, *Shock-Wave Phenomena in Condensed Media* ("Yanus-K", Moscow, 1996) [in Russian].
21. M. A. Il'gamov, V. A. Ivanov, and B. V. Gulin *Strength, Stability, and Dynamics of Shells with Elastic Filler* (Nauka, Moscow, 1977) [in Russian].
22. I. F. Ostriuk, I. B. Petrov, and V. P. Petrovskii, "Computation of Strain of an Acoustic Pulse of Small Duration on a Hole of Complicated Shape in a Filler in an Elastic Shell," *Mat. Modelirovanie* **2** (8), 51–59 (1990).